NASA
Technical
Paper
2394
c.2
November 1984

A Preliminary Study of Numerical Simulation of Thermosolutal Convection of Interest to Crystal Growth

Timothy L. Miller

NASA

NASA Technical Paper 2394

1984

A Preliminary Study of Numerical Simulation of Thermosolutal Convection of Interest to Crystal Growth

Timothy L. Miller

George C. Marshall Space Flight Center
Marshall Space Flight Center, Alabama

National Aeronautics and Space Administration

Scientific and Technical Information Branch

TABLE OF CONTENTS

LIST OF ILLUSTRATIONS

TECHNICAL PAPER

A PRELIMINARY STUDY OF NUMERICAL SIMULATION OF THERMOSOLUTAL CONVECTION OF INTEREST TO CRYSTAL GROWTH

I. INTRODUCTION

Thermosolutal (or "double-diffusive") convection shall refer, in this work, to buoyancy-induced convection where there are two or more density components (e.g., heat and solute). The most interesting cases are when the diffusivities of the separate components are very different from each other. In the most common example (heat and salt), the diffusivities differ by a factor of about 100, heat having the higher diffusivity. This results in some perhaps surprising phenomena – in particular, the instability of a quiescent fluid which is bottom-heavy and which has no horizontal density gradients.

The two simplest situations (continuing with the heat/solute example) are those in which there are no horizontal gradients of either component, and where one component contributes to a stable stratification while the other component contributes to an unstable stratification. For the purposes of discussion, it is assumed that the overall density increases downward (i.e., the fluid is bottom-heavy). If no double-diffusive effects are considered, a fluid element displaced vertically would have a force exerted upon it which would restore it to its initial position. Due to dissipation, it would arrive there with less momentum (and buoyancy) than it started with. Thus, vertical motions are damped and no instability would arise. However, if the more slowly-diffusing component contributes to a top-heavy state, a phenomenon, called "salt fingers," can occur. Since the diffusivity of heat is very large compared with that of the solute, the vertically displaced element tends to "feel" the destabilizing buoyancy effects of the solute rather than the effects of temperature. That is, the fluid element finds that it is quickly heated (or cooled) to the approximate temperature of its new environment, but that it has a different density than its environment due to its solutal concentration, which remains approximately the same as the original value. Thus, its vertical displacement is accelerated rather than damped. This instability consists of vertically long convection cells with small horizontal extent (hence the name "salt fingers"). The second situation is when the fluid is stable with respect to the more slowly diffusing component (solute), and unstable with respect to temperature (i.e., hot at the bottom). A vertically displaced fluid element will be buoyantly restored toward its initial position (due to the stable stratification of the solute) and will arrive there with essentially the same solutal concentration with which it left; but because of the relatively high diffusivity of heat, after it arrives back at its original position the fluid element finds itself either warmer (if the initial displacement was downward) or cooler (if the initial displacement was upward) than it was originally. Hence, an amplifying oscillation develops, most often called the "oscillatory" or "diffusive" instability. The appearance of this type of convection is usually that of horizontal layers of convection cells; but this form is much more complex than the finger convection, and the number of layers within a given vertical depth depends upon initial and boundary conditions and may be time dependent [1].

It is reasonable to expect that thermosolutal effects may be important in crystal growing situations where there exist density gradients in the fluid feed material due to both temperature and solutal concentration gradients, and that in some cases any theoretical model which neglects these effects is omitting some fundamental physics. The crystal growing situation that shall be used as our "typical" system here is the Bridgman-Stockbarger method, whereby a substance in a long cylindrical ampoule is held vertical and moved downward through a furnace with highly controlled temperature conditions. The substance is thus solid (crystalline) below a hot melt. A basic axial (vertical) temperature that is buoyantly stable is thus imposed upon the melt, the lower surface being approximately isothermal (at the melting point temperature). The

substance under process is often made of two components. One of the components (the "solute") tends to be rejected at the interface and incorporated into the solid less readily than the other substance (the "solvent"). Thus, an axial gradient in solute may exist in the system. If the solute is lighter than the solvent, it is speculated that the "finger" process may give rise to that simplest form of thermosolutal convection. A linear analysis of this situation is performed in Reference 2. Additionally, radial (horizontal) gradients in both temperature and concentration may induce convection, which may be expected to be influenced by the double-diffusive nature of the system. For example, even when the solute is heavier than the solvent, horizontal temperature gradients combined with the stable concentration profile may give rise to horizontal layers such as those observed by Thorpe et al. [3] and Chen et al. [4] in a heat/salt system. The presence of these layers, with very narrow regions of large gradients, would make the numerical modeling of the fluid motions quite challenging [5,6,7]. The modeling of the fluid motions is important in order to predict the characteristics of the crystal itself – for example, the concentration of solute ("dopant") in the crystal may have important radial variations if cellular convection is present, and axial variations if the flow is time-dependent.

Rather than give an extensive review of research in thermosolutal convection in general, this report refers the reader to the references herein, especially Chen and Johnson [8], which is a review article of a conference on the subject in the spring of 1983. Most of the work has been done under the auspices of oceanographic research beginning in the 1960's (actually, the first work on it was Stommel et al.,[9]), and a rather sparse scattering of experimental, observational, analytical, and numerical work has been done. Some of the work that has been done on numerical modeling of thermosolutal convection, with particular emphasis placed upon applicability to crystal growth, is reviewed here.

The linear stability of a quiescent state has usually been handled by purely analytical methods, the computer being used only for the purpose of displaying the results. Although not discussed here, some of this work is included in the bibliography [10,11,12]. Veronis [13,14] and Sani [15] were the first to compute fully nonlinear thermosolutal convection. They did so for the oscillatory situation between horizontal flat plates (the infinite channel) which has limited applicability to crystal growth. However, it is interesting to note that in some instances finite amplitude disturbances were found to be unstable even when the thermal driving was subcritical – i.e., when the system was stable to the infinitesimal disturbances of linear theory. Huppert and Moore [16] extended the work of Veronis to give more details about the type of flow expected as a function of the parameter combinations. Their work and the work of Moore et al. [17] indicate the complexity of the system, even when values of the diffusivities involved are not as extremely different as would be expected in physical situations. The finger system is less complex, but still difficult to model numerically for all but the highly idealized systems. Straus [18] used a Galerkin technique to study fully nonlinear finger convection between horizontal plates. He made progress toward reconciling the fact that observations of the cells indicated much shorter wavelength than that predicted by linear theory. He found that only small-scale motions are themselves stable, and that the most stable convection cell has a wavelength which is approximately the same as that which maximizes the flux of solute. The present author has been unsuccessful at finding previous calculations of either type of convection in an enclosed container.

As indicated earlier, there have been previous calculations performed of a system with horizontal temperature gradients imposed upon a fluid in a container which is initially stably stratified with a salt gradient [5,6,7]. These calculations met with limited success. From their figures it can be seen that the spatial resolution was not adequate, since a spatial computational mode ("wiggles") is apparent. The calculations were successful, however, at predicting the horizontal layering that occurred in the laboratory experiments, including the correct wavelength. The difficulty lies in the fact that the horizontal convection cells have very strong shear between them, with accompanying strong gradients over narrow regions in the temperature and concentration fields. Thus, high spatial resolution is required to resolve all the fields (especially concentration) – resolution which is not practical to use, except perhaps on today's super-computers (not available to the previous workers).

Calculations of crystal growth fluid dynamics have not yet been made with full allowances for thermosolutal effects, although there is work presently being done in this area by groups at MIT (under the direction of R. A. Brown) and at the National Bureau of Standards. (F. M. Carlson [19] at Clarkson College has considered purely thermal convection.) At NBS, G. McFadden and S. Coriell (Schaefer et al., [20]) have performed calculations of melt flow including thermosolutal effects where there is a crystal "growing," but the presence of sidewalls and interface curvature are neglected (i.e., a horizontally infinite channel is considered). A finite difference method is used, and a computational domain is chosen such that one complete wavelength in the horizontal is resolved, and such that the upper horizontal boundary is far enough from the flow (which is present due to the unstable boundary layer at the interface – the lower boundary) that there is approximately no influence from it. A growth rate is imposed, and due to a nonzero segregation coefficient, (light) solute is rejected at the interface. The heat flow due to conduction is calculated in the solid crystal below. This work is an extension of the infinite channel work noted above, the primary difference being that the basic temperature and solute fields are exponential, rather than linear, due to the imposed growth rate and boundary conditions. "Salt finger" convection is predicted for certain parameter combinations, and the NBS group has investigated such questions as the vertical extent of the convection, the solute and heat fluxes, and the horizontal wavelength at which the convection cells split into two. No attempt has been made to determine the wavelength at which the convection is most vigorous in some sense (such as maximum solute transport). The recent published work by the MIT group [21,22] has made the transition from calculations of crystal growth including convection due to temperature gradients only to that with solutal buoyancy effects as well. Calculations are performed in a cylindrical domain, and include the heat flow in the solid crystal as well as the calculation of the interface shape. The sidewall boundary conditions on temperature in the fluid domain are those of no heat flux for a given distance near the interface, and isothermal above that. The convection studied is due to the radial (horizontal) temperature gradients that are present because of this discontinuous boundary condition; the convection is either enhanced or suppressed by the solute, depending on whether it is light or heavy. This is not thermosolutal convection in the sense described above, since there is no qualitative change in the flow due to the presence of the solute. The fact that the flow (except for the parallel flow due to the crystal growing) is due entirely to the discontinuous boundary condition, makes detailed study of it of questionable relevance to actual crystal growth, where heat flow in the ampoule may cause the boundary conditions in the fluid region to induce an entirely different (surely quantitatively if not qualitatively) flow than that studied by the MIT group. It should also be noted that the diffusion parameters and density variations used by the MIT group are not nearly as extreme as those of the actual physical situation, and thus thermosolutal effects such as fingers or horizontal layering were effectively excluded.

The present work is considered to be preliminary results of an effort to study thermosolutal convection of particular interest to crystal growth by means of numerical models. Finite difference methods are used, the models being adapted from those used to study laboratory experiments and the infinite channel in geophysical fluid dynamics [23,24,25]. Since explicit time differencing is used mainly, computer resources required are rather large – the primary reason these results are "preliminary." Section 4 (Finger Convection in the Infinite Channel) describes some progress toward making the codes more efficient. After the improvements are completed, research will be oriented toward areas that results have shown to be the most promising for further study. There are three areas studied: (1) horizontal heating of a stably stratified solution; (2) finger convection in a box, in some cases with the inclusion of a horizontal temperature gradient on the bottom surface; and (3) finger convection in infinite channel geometry.

II. SIDE-HEATED CASES

The calculations reported in this section relate to the laboratory results of Thorpe et al. [3], Chen et al. [4], Wirtz et al. [5], and Hart [26] – and, to a lesser extent, to Ruddick and Turner [27]. In the first

four works, a box is filled with a salt solution, the concentration of which decreases linearly upward (i.e., the fluid is made bottom-heavy). One of the side walls is then heated, and the other held at a fixed (lower) temperature. In References 3 and 26, the heating is done very slowly; one purpose being to allow a basic flow to become established with a horizontal gradient in solute concentration, which approximately compensates for the horizontal gradient in temperature. In the vertically infinite situation, there exists a known steady basic state – an exact solution to the full equations where there are no vertical variations in the velocities, temperature, or the solute gradient. This situation can be approximated by a very tall, narrow slot in the laboratory. The experiments by Chen et al. and Wirtz et al. (these two works are by the same group) had the temperature of the heated side wall rise very fast (with an e-folding time of about 3 min). The problem in this case is that of the stability of a time-dependent flow near a single vertical wall. The work by Ruddick and Turner [27] was a set of laboratory experiments where a sugar solution was beside a salt solution (both stably stratified), and the partition between them was carefully removed. In all of the side-heated cases, appropriate parameter combinations resulted in a flow with horizontal layers, where each layer consisted of a convection cell of thermally direct rotation, with very strong shear between them. The development of cells began near the heated side wall, and the cells would eventually extend across the width of the volume. The theory of Hart [26,28] explained very well the slowly-heated tall slot, and a simple theory explains the vertical depth of the layers in the rapidly side-heated case [4]. Chen [29] numerically studied the linear stability of the time-dependent parallel flow in the latter case, with good success in predicting the critical wavelength and Rayleigh number. Even though the flow is essentially two-dimensional, numerical modeling of the fully nonlinear flow is difficult (even when cases with only a few layers are considered), because the strong shear between layers and the low diffusivity of the solute results in the need for very high resolution. Another difficulty that can arise is due to the observations (and predictions by the theory of Holyer [30]) that the layers themselves may become unstable to finger and diffusive convection. The finger convection, especially, places an even more severe constraint on the resolution required to describe the flow. An attempt to avoid cases where this might occur was made in the present work, although it may be seen that the resolution, while somewhat greater than that used in previous works (except, in a sense, for Wertz et al., [5]), was evidently inadequate in some cases, and perhaps with finer resolution these detailed features would have been predicted.

This report shall consider two-dimensional flow of a fluid in which the Boussinesq approximation is valid. z is taken to be the vertical coordinate and y to be the horizontal coordinate. If the two components of the momentum equation are cross-differentiated, a vorticity equation is derived:

$$\frac{\partial \zeta}{\partial t} = \frac{-\partial \psi}{\partial z}\frac{\partial \zeta}{\partial y} + \frac{\partial \psi}{\partial y}\frac{\partial \zeta}{\partial z} + g\frac{1}{\rho_o}\frac{\partial \rho}{\partial y} + \nu \nabla^2 \zeta \quad , \tag{1}$$

where ν is the kinematic viscosity and where the stream function is related to the vorticity by:

$$\nabla^2 \psi = \zeta \quad . \tag{2}$$

The velocity components are related to the stream function by:

$$\frac{\partial \psi}{\partial z} = v \quad ; \quad \frac{\partial \psi}{\partial y} = -w \quad . \tag{3}$$

The equations describing the evolution of the temperature and solute concentration fields are, respectively:

$$\frac{\partial T}{\partial t} = \frac{-\partial \psi}{\partial z}\frac{\partial T}{\partial y} + \frac{\partial \psi}{\partial y}\frac{\partial T}{\partial z} + \kappa \nabla^2 T \tag{4}$$

$$\frac{\partial C}{\partial t} = \frac{-\partial \psi}{\partial z}\frac{\partial C}{\partial y} + \frac{\partial \psi}{\partial y}\frac{\partial C}{\partial z} + D\nabla^2 C \quad , \tag{5}$$

where κ is the thermal diffusivity and D is the solutal diffusivity. Density shall be taken to be a linear function of temperature and solute concentration:

$$\rho = \rho_o[1 - \alpha(T - T_o) + \beta(C - C_o)] \quad , \tag{6}$$

where α and β are the thermal and solutal coefficients of expansion, respectively. In this section, boundary conditions on temperature shall be taken to be of the Dirichlet type on the side walls (i.e., they are assumed to be perfect conductors), and the horizontal end walls will be perfectly insulating. In some cases the temperature of the hot wall will be brought up exponentially (with time), and in others it will be fixed throughout the integration. The side walls, and in some cases the end walls as well, shall be taken to be zero-flux walls with respect to the solute. There are some cases where the end walls have fixed solutal concentration imposed upon them. No-slip boundary conditions are used in all cases.

If the equations are non-dimensionalized, the dimensionless parameters that appear are the thermal and solutal Rayleigh numbers, the Prandtl number, and the Schmidt number. Aspect ratio also appears after the spatial domain is defined. These are defined:

$$Ra_T = \frac{g_\alpha \Delta T L^3}{\nu\kappa} \tag{7}$$

$$Ra_S = \frac{g\beta \Delta C L^3}{\nu\kappa} \tag{8}$$

$$Pr = \nu/\kappa \tag{9}$$

$$Sc = \nu/D \tag{10}$$

$$\gamma = \frac{\text{height}}{\text{weight}} \tag{11}$$

A finite difference technique is used to solve the equations. The domain (a vertical plane) is sectioned into a grid – not necessarily of uniform grid element size, but one where the resolution may gradually increase near the boundaries. The equations are finite differenced in explicit centered form, although because of the grid stretching the spatial differencing is not truly centered (i.e., second order). (A variable transformation scheme is not used.) Details of the technique are in Miller and Gall [23,24]. The technique was shown to be valid by reproducing in detail a laboratory transition curve between axisymmetric and non-axisymmetric flow for the baroclinic annulus. Furthermore, axisymmetric calculations of thermally-driven flow (rotating and non-rotating) in an annulus agree quite well with those of previous workers. The necessary addition to the Miller and Gall code was simply to add the solute concentration field to the problem. After calculating the temperature, concentration, and (interior) vorticity fields at a given time step, the finite differenced equation (2) is solved either by direct Gaussian elimination (for the abruptly-heated cases) or by successive line over-relaxation (SLOR). (The latter technique proved to be too inefficient when the stream function had rapid change over a small region.) The no-slip boundary condition on the stream function (normal derivative equals zero) is imposed when the boundary value for vorticity is then calculated. The initial conditions are that there is no motion in the fluid volume. Computer time required on the VAX 780 for the resolutions here is about 30 min per 1000 time steps.

The rapidly-heated side wall case shall be discussed first. This case uses the no-flux boundary condition on solutal concentration on the entire boundary. (Note that when this is the case, the only true steady state is one where there are no solutal gradients in the fluid volume – eventually, the flow will mix the solute throughout the fluid.) Chen et al. [4] reports that the initial rise of temperature of the side wall could be modeled by an exponential function $\Delta T(1 - e^{-t/\tau})$, where τ is about 2 min. Thus, the code was modified to allow for this; i.e., the temperature that was imposed upon the hot wall (the other one being fixed for all time) rose exponentially, with an exponential rise time of either 2 min (cases 1 and 2) or 3 min (case 3). The initial condition for the interior was of constant temperature – that of the "cold" wall.

Chen et al. points out that the distance L that a fluid particle, within a basic density gradient $\phi_o = \beta\, \partial C_o/\partial z$, receiving a temperature increase of ΔT, will rise before it is in a neutral buoyancy environment, is:

$$L = \frac{\alpha\, \Delta T}{\phi_o} \quad .$$

It is expected that the vertical spacing between layers will be of this scale, and this is verified experimentally. Chen et al. uses this L as the length scale in defining the dimensionless parameters, and so will we. The dimensions of the computational domain in this report are referred to in terms of this L.

It is noted that the experimental results were for many layers (on the order of 100). It is not realistic to numerically model this situation under the present circumstances (explicit methods, small computer). Thus, the attempt was to model cases where one would expect five or fewer layers. Results are given here for cases with one to four layers. Note that Wirtz et al. [5] performed limited calculations (the integrations were performed only until the layers were just beginning to develop) for a case with about eight layers, and Wirtz [7] performed calculations for cases with only one and two layers. The relevant numerical and physical parameters used here are given in Table 1.

The vertical extent of case 1 (Fig. 1) was 5L, and the horizontal extent was 3L. (The dimensions were 3 cm by 5 cm for this case, and 2 cm by 3 cm for all other cases in this section.) The diffusivities were the actual ones of heat and salt, and the viscosity was that of water. The resultant Prandtl number was about 7, Sc = 714, $Ra_T = 5 \times 10^4$, and $Ra_S = 1.5 \times 10^5$. Initially, as the temperature difference is brought up

TABLE 1. RELEVANT NUMERICAL AND PHYSICAL PARAMETERS

Case	Ra_T	Ra_S	Height	Pr	Sc	Time step	Grid	Total Time
1	50,000	150,000	5L*	7.14	714	0.03 sec	32 x 31	285 sec
2	10,000	30,000	3L	7.14	714	0.03 sec	32 x 31	450 sec
3	40,000	40,000	1L	7.14	714	0.03 sec	32 x 31	600 sec
4	21,000	63,000	3L	7	10	0.05 sec	30 x 28	300 sec
5	4,200	12,600	3L	7	625	0.05 sec	30 x 28	2700 sec
6	2,940	8,820	3L	1	10	0.05 sec	30 x 28	215 sec

*Height is given in terms of the buoyancy length $L = \alpha \Delta T/\phi_o$. Dimensional size of L was 1 cm for all cases, and viscosity was 1 centistoke.

from zero there is a single cell throughout the volume (Fig. 1a), although it may be seen in the figure that cells are beginning to break off in the lower and upper corners near the heated wall. Note that the time has been so short (35 sec) and the velocities so small (about 10^{-3} cm-sec^{-1}) that a fluid particle has moved only a very small fraction of the total height. At a later time (142 sec) an intense cell has developed in the lower, hot corner. This is as observed in the experiments. A weaker cell is evident near the upper boundary. After 285 sec, two layers between the corner circulations are beginning to form, resulting in four layers. Although five layers were expected, it is noted that the experimental result was that the thickness of the layers was only approximately L, and also that the corner circulations change the basic temperature and solutal fields from the original one. At this point in the integrations, however, it is evident from the solutal concentration field (and even more so for the field of vertical density derivative, not shown) that resolution is not adequate, because there are wiggles which correspond to every other grid point. An upstream differencing scheme was tried for the solutal equation, and although this resulted in smoother fields, it did not predict the layering and thus was even more undesirable.

Case 2 (Fig. 2) was for thermal and solutal Rayleigh numbers one-fifth those in case 1. (This is a sub-critical case, according to the laboratory results.) There is a strong circulation in the lower warm corner, but layers that would be identifiable in the lab are not apparent. Yet still there are indications in the solutal concentration field that resolution is inadequate. Case 3 (Fig. 3) is for a case with height equal to 1L, and the thermal Rayleigh number is equal to 4×10^4. The circulation is qualitatively like one computed by Wirtz [7], although it is integrated here for a longer time period. Obviously, the resolution is inadequate, although the temperature field and the general shape of the flow are quite reasonable.

Calculations were also performed with more idealized parameters, looking for interesting flows that could be well resolved using the present techniques and computer. Case 4 (Fig. 4) has $Ra_T = 21{,}000$ and height 3L. Prandtl and Schmidt numbers were 7 and 10, respectively. Besides the much higher solute diffusivity, this case also differed from the previous ones in that the temperature of the hot and cold walls were fixed for all time, and that the initial condition for temperature was that of a linear gradient between the two walls. Thus, the problem was symmetric with respect to the hot and cold wall. The boundary condition on solute concentration was again no-flux for all surfaces, and the flow shown is quasi-steady. There are only two layers present, one circulation centered near the lower hot wall and another near the upper cold wall. The circulation is such that the concentration and temperature fields are adjusted so that the density contours in the interior are nearly horizontal. Note that qualitatively this flow is very similar

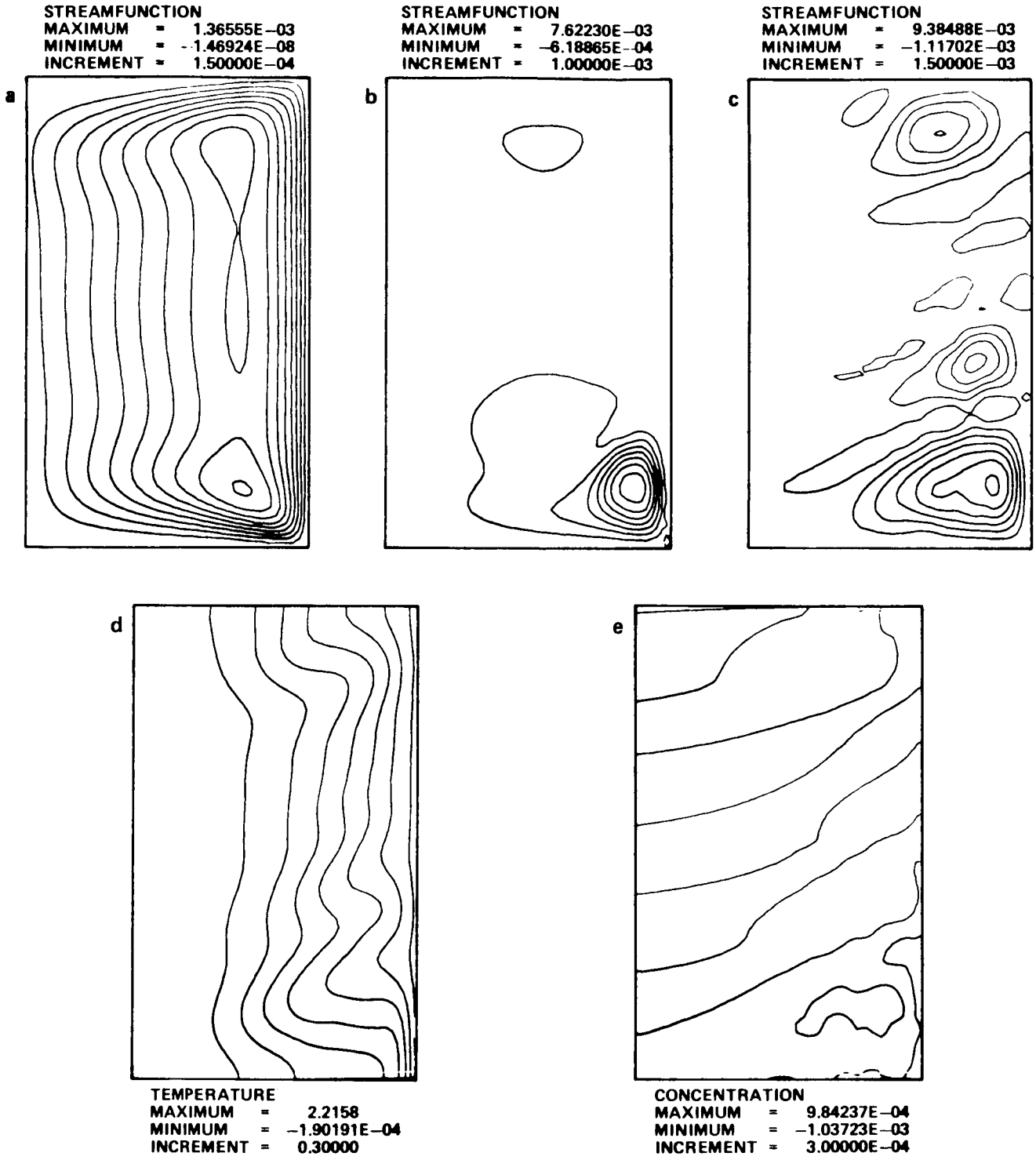

Figure 1. Results of calculations for case 1 of Section II (see Table 1). (a) Stream function at 35 sec. (b) Stream function at 142 sec. (c), (d), and (e): Stream function, temperature, and concentration at 285 sec. Stream function value should be divided by 500 in Figures 1 through 12.

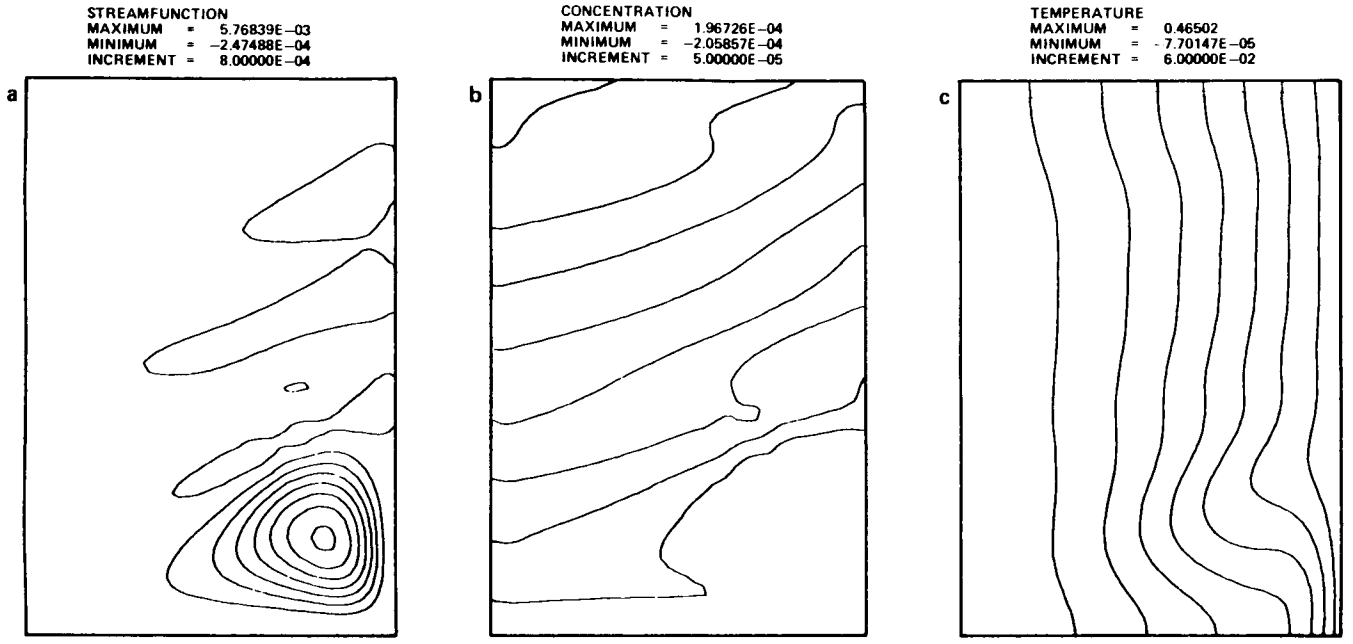

Figure 2. Results of calculations for case 2 of Section II (Table 1) at 450 sec.

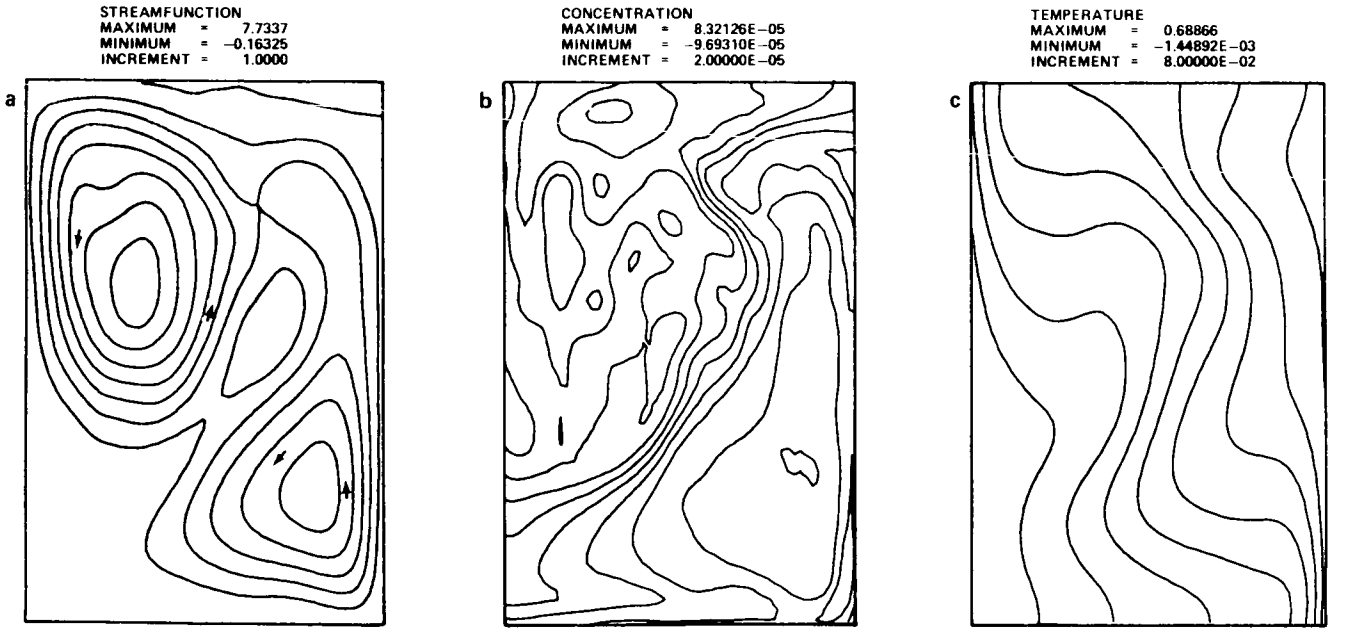

Figure 3. Results of calculations for case 3 of Section II (Table 1) at 600 sec.

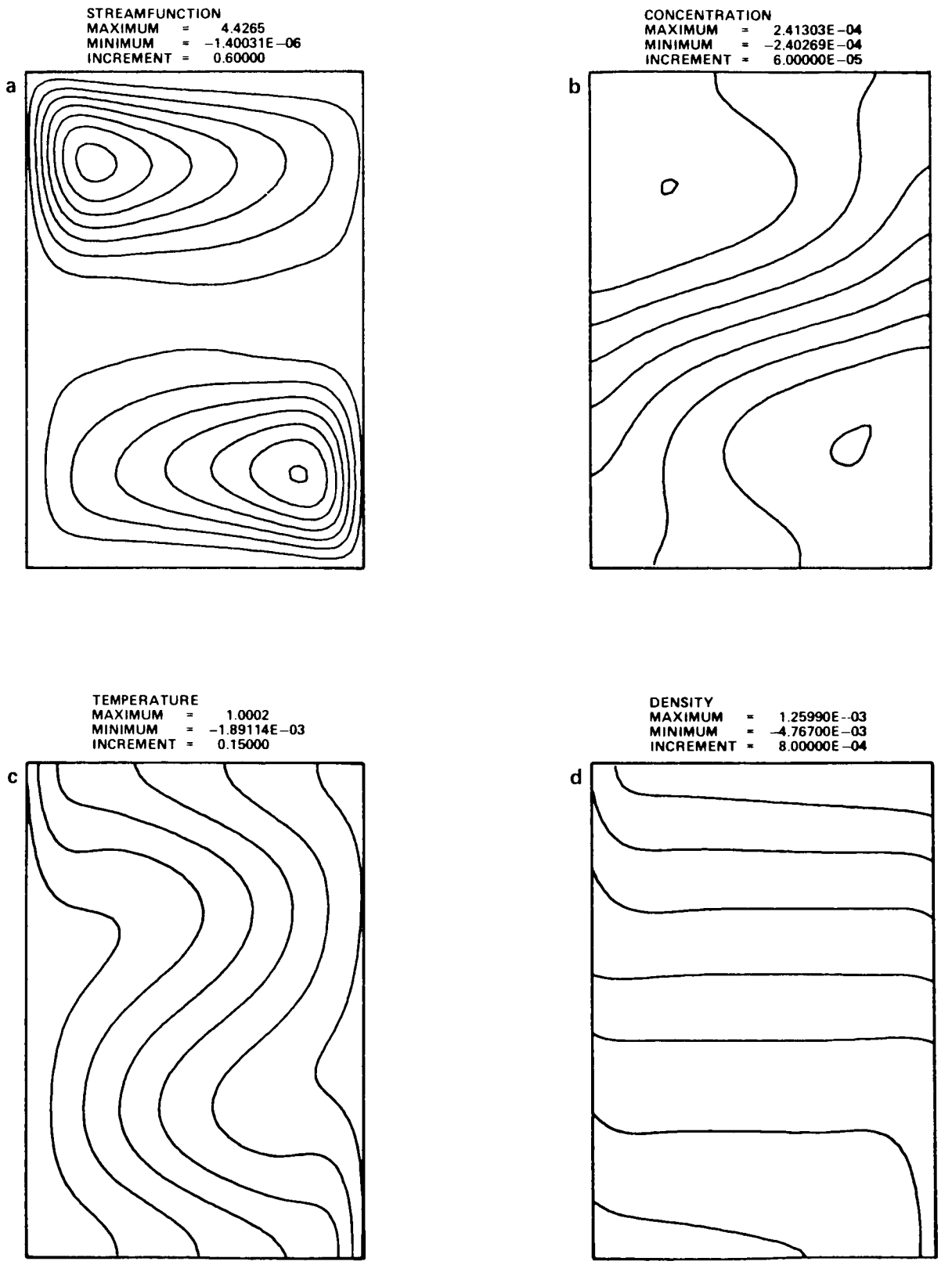

Figure 4. Results of calculations for case 4 of Section II (Table 1) at 300 sec.

to one of the cases computed by Wirtz [7], the main difference being that Wirtz used a Schmidt number of 1000 (that for salt), and he had a resolution problem because of it. Some of his comments regarding the physical significance of the fine structure of the solutal field are not well substantiated, since the fine structure is not resolved by the grid and may be numerical rather than physical.

Case 5 (Figs. 5 and 6) is for a Schmidt number of 625 and $Ra_T = 4200$, other parameters being the same as for case 4. The boundary conditions on solute at the top and bottom are of fixed concentration. (This means that a steady state, which retains the solutal stratification, is possible.) At 300 sec there are again the two circulations at the bottom near the warm wall and at the top near the cool wall. Here, these circulations are much more separated (i.e., of smaller vertical extent), a consequence of the lower solutal diffusivity. Since solute is more nearly conserved, the buoyant restoring force is effectively stronger, and a fluid particle rising (sinking) because it is heated (cooled) does not go as far before turning inward. Note that again the interior isopycnals (Fig. 5d) are approximately horizontal.

After a very long time of integration (2700 sec), the solution has not completely converged, but changes occurring are quantitative only and are occurring very slowly. There are three convective layers (Fig. 6), the middle one becoming substantial in the contour plot at about 1200 sec. It is hypothesized here, although not argued on precise theoretical grounds (this would be future work), that the 3-layer flow resulted out of the instability of the flow pictured in Figure 5. The solutal and thermal Rayleigh numbers, as defined by Hart [28] for this case, are very near the critical curve (on the unstable side) for the vertically infinite slot. It is reasonable to hypothesize the possibility that a basic state would be able to develop when one is so near the critical curve; and that although the present system is very far from being an infinite slot, the critical curve for this system may not be too far from the idealized one. Note that the fields are fairly well resolved, although the solute concentration field does exhibit a weak computational mode, indicating that resolution should be better.

Perhaps the most interesting case is depicted in Figures 7 and 8. This is case 6, and is for $Ra_T = 2940$, $Pr = 1$, $Sc = 10$, and height equal to 3L. The concentration is fixed at the top and bottom, as in case 5. The flow is vacillating between a single-cell thermally direct (counter-clockwise) circulation and a thermally indirect circulation. These circulations and the transitions between them are shown in the sequence of stream function plots in Figure 7. Note that a positive stream function value implies a counte-clockwise flow and that a negative stream function value indicates a clockwise flow. The transition between single cell flow is characterized by a break-down of the single cell into multiple cells and an expansion and eventual merging of cells of the opposite rotation (opposite from the previous single cell flow). The thermally direct cells form and expand from the lower hot and upper cold corners. The thermally indirect cells do likewise from the interior. The pattern shown here repeated itself several times, and the amplitude of the oscillation (in, say, kinetic energy with time) seemed to be rather constant. Further work is needed for a definitive demonstration that this is indeed vacillation (i.e., that it will never become a steady flow).

Figure 8 shows the temperature and concentration fields at time 203 sec and density field at time 203 and 200 (similar to that at 212) sec. The temperature contours remain rather vertical; the concentration field approximately compensates for the horizontal temperature gradient so that the net horizontal density gradient is small. It is evidently the small deviation from no horizontal gradient, however, that drives the vacillation. Note the opposite tilt of the isopycnals in Figure 8c and 8d. In Figure 8d, the circulation is near its counter-clockwise peak, and the isopycnals are nearly horizontal. The circulation advection quickly causes a tilt of the interior isopycnals so that there is a reversing torque (Fig. 8c), and an opposite circulation develops which eventually tilts the isopycnals in the opposite direction (not shown), again reversing the torque. This process is perpetuated by the boundary conditions, which cause the persistance of a horizontal density gradient in the lower hot and upper cold corners. It may be hypothesized

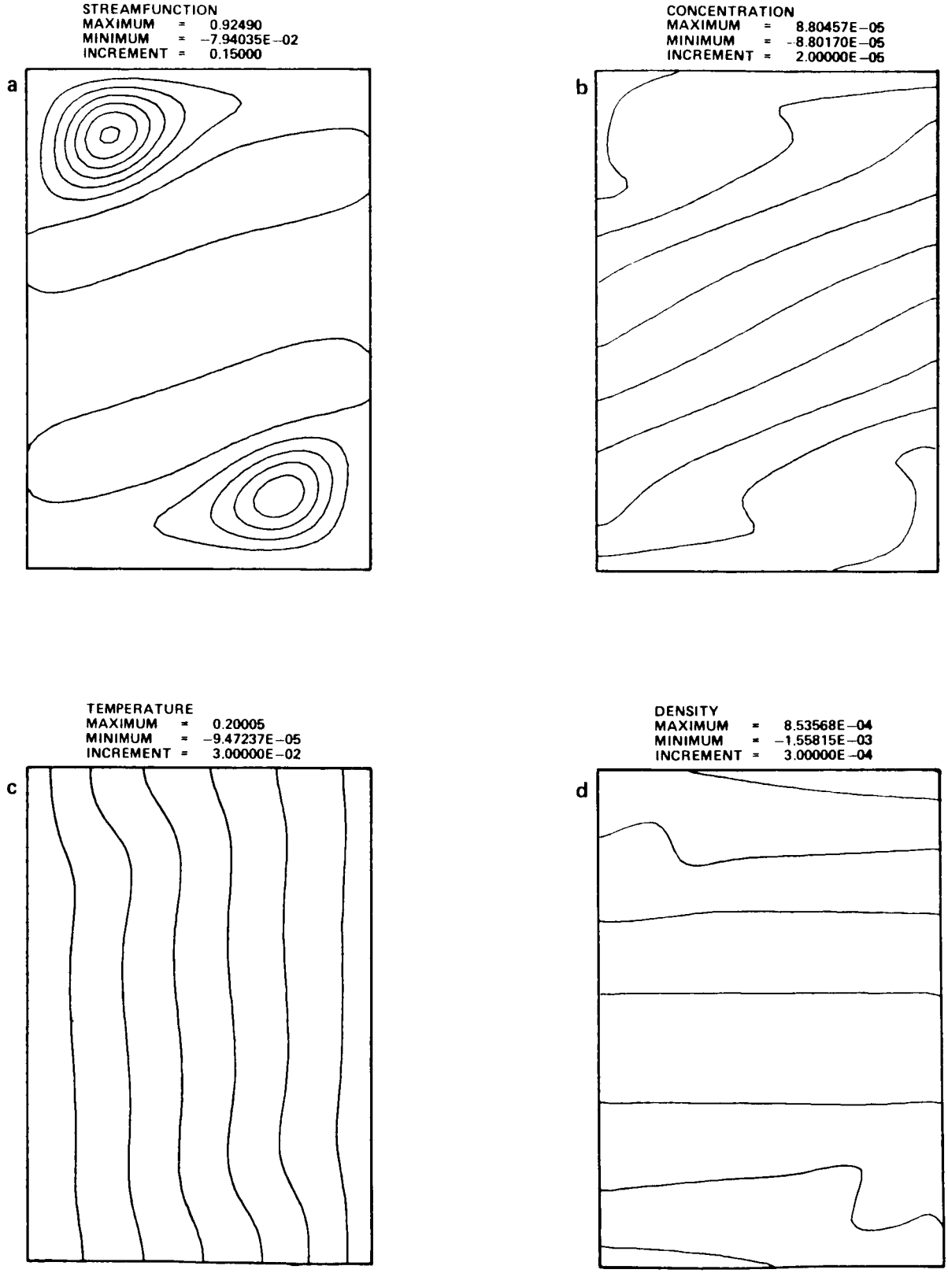

Figure 5. Results of calculations for case 5 of Section II (Table 1) at 300 sec.

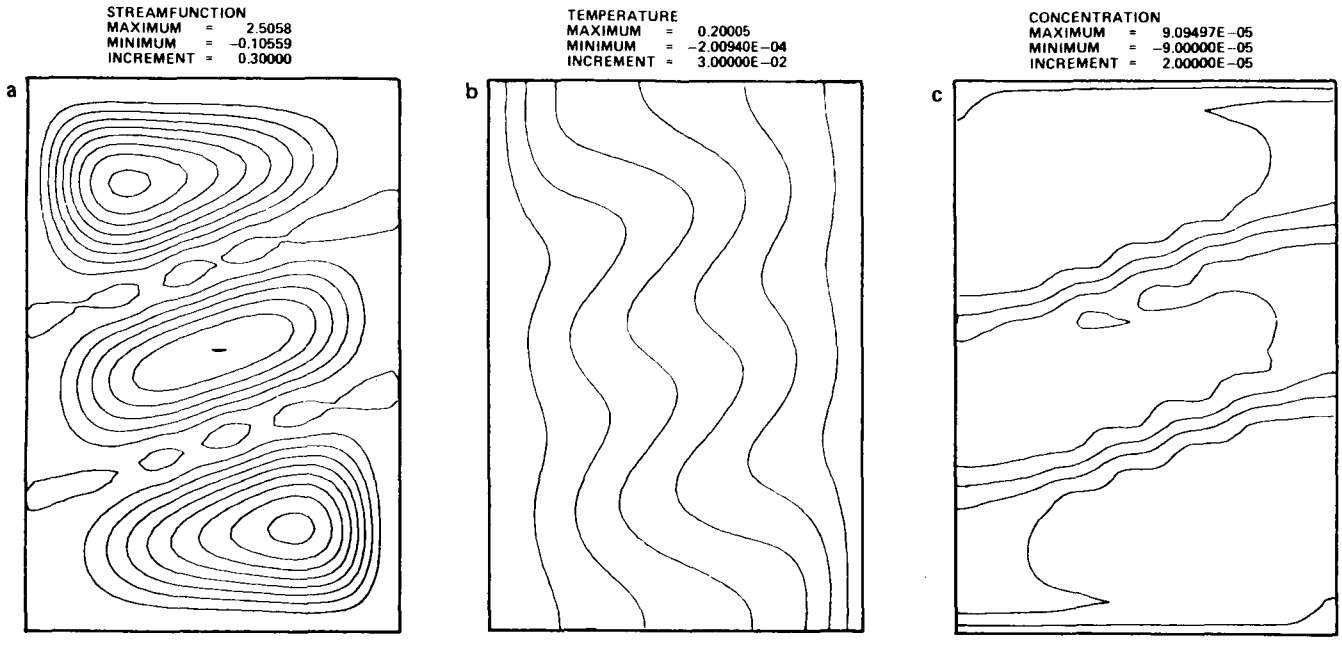

Figure 6. Results of calculations for case 5 of Section II (Table 1) at 2700 sec.

that there exists, as a solution to the equations, a weak thermally direct circulation, but that it is not seen because it is unstable. It is also possible, as previously suggested, that if this integration were carried out much further the vacillation would go away. This is a specific area where further work would be interesting.

In conclusion, although some very interesting and informative work can be done with the present spatial resolution for idealized parameters, to accurately model the laboratory experiments will require much higher resolution. This work indicates that if similar types of flow exists in crystal growing systems (and it is reasonable to expect so), then the resolution required to model the flow in the melt and to therefore accurately calculate such quantities as dopant segregation will be quite large; it is likely that super-computers such as a Cray or the Cyber 205 will prove to be useful (in fact, necessary) for this task.

III. FINGER CONVECTION IN A BOX

The same model, described in the previous section, was used to calculate some flows where the vertical gradient in the temperature field was in the stable direction and the solute gradient was destabilizing. The boundary conditions on temperature and concentration were of fixed value on the upper and lower boundaries and of no flux on the side boundaries. No-slip boundaries are assumed, and the same dimensions (2 cm by 3 cm) and viscosity as in the previous section were used. When there were no horizontal gradients imposed, a very small random perturbation in the concentration and temperature fields was added to the initial condition, which was that of diffusive equilibrium and no flow. Some of the cases have horizontal temperature gradients on the bottom, which is analogous in a certain sense to a curved interface in crystal growth. An interface may be curved, for example, when the thermal conductivity of the solid below the melt is significantly less than that of the melt. The heat must flow downward, and in order to do so some

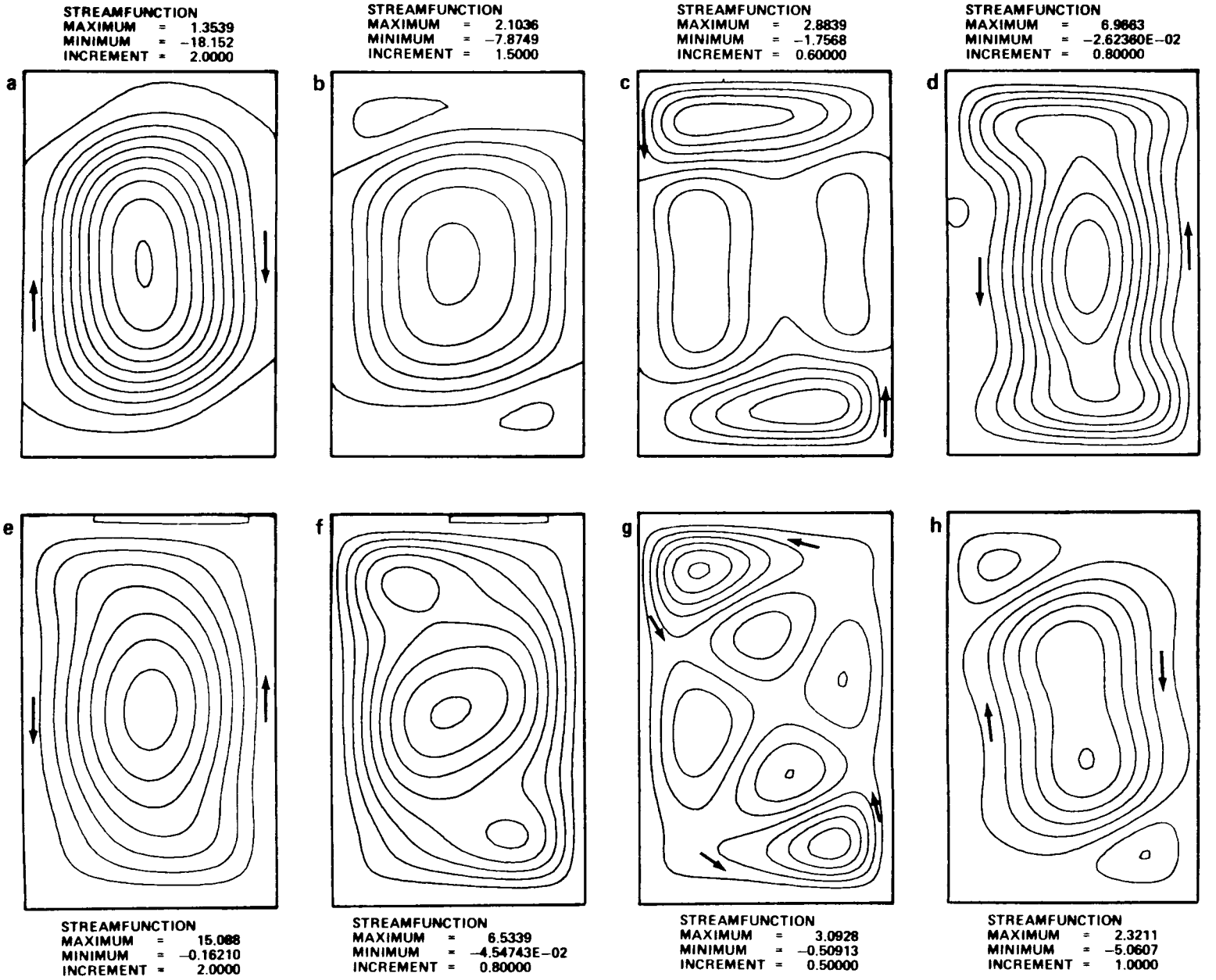

Figure 7. Calculated stream function for case 6 of Section II (Table 1) at various times. (a) 206 sec, (b) 209 sec, (c) 210 sec, (d) 211 sec, (e) 213.5 sec, (f) 216 sec, (g) 217 sec, and (h) 218 sec.

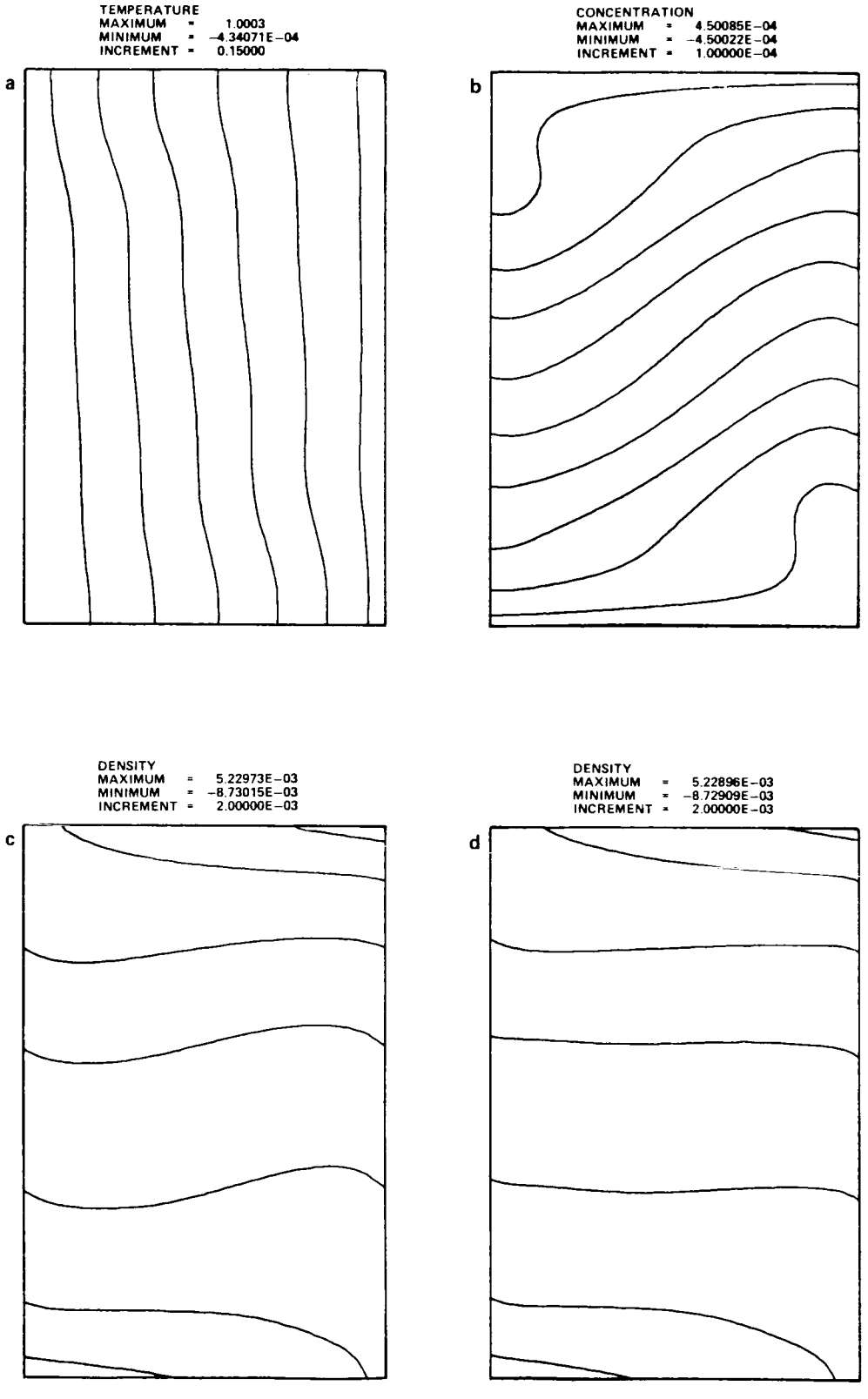

Figure 8. (a), (b), and (c): Calculated temperature, concentration, and density fields for case 6 of Section II at 203 sec. (d) Calculated density field at 200 sec.

of it must be conducted through the ampoule (side wall). This requires the presence of horizontal temperature gradients and hence a curved interface, since it is approximately isothermal.

Although no theory has been developed for the stability of the finger situation when side walls are present, the critical solutal Rayleigh number can be approximated by consulting the infinite channel theory. Case 1 (Fig. 9a, b, c) is for $Ra_S = -1.2 \times 10^5$, $Ra_T = -8.3 \times 10^5$, Pr = 1, and Sc = 10, where the total height (3 cm) was used for the length scale in the Rayleigh numbers. Using the free-slip infinite channel theory (Baines and Gill, [31]), the critical solutal Rayleigh number, given the other parameters, is -8.3×10^4. This case is expected to exhibit an instability, but it would not be very strong. The flow depicted was integrated for 1050 sec, and is still evolving (growing in amplitude). Being relatively near the critical curve resulted in the growth rate of the instability being small and hence taking a long time for the convection to become the amplitude seen in the figure. There are one and one-half complete horizontal wavelengths contained within the volume. The advection effects upon the solute are strong, but the effects upon the temperature field are rather small.

Case 2 (Fig. 9e, f, g) was for the same parameters as the previous case, except that the Schmidt number was 25. Hence, the critical Ra_S was -3.3×10^4, and the Ra_S was about four times critical. The flow was much stronger, the wavelength smaller, and the instability arrived faster. The fields shown in the figure for this case are also still evolving.

If there is a horizontal gradient imposed upon the lower surface and no solutal effects are considered, a single thermally direct cell is induced (case 3, Fig. 10). Because the horizontal driving is only on the lower surface and because of the imposed vertical gradient, the circulation is confined to the lower region of the volume. Some calculations were performed to test the effect that the addition of this circulation would have upon the pure salt finger cases described above. Case 4 (Fig. 11) is with the horizontal gradient added to case 1, and case 5 (Fig. 12) is with the same horizontal gradient added to case 2. The addition of this lower circulation seemed to "kick off" the finger convection faster than with the quiescent basic state. The overturning, which tends to stabilize the basic state in the pure thermal convection case, did not seem to perform an analogous function here. None of the cases here (except the pure thermal case) were integrated to steady state, and it is possible that cases 1 and 2 would eventually have become more vigorous than cases 4 and 5. It is important to point out that the horizontal temperature gradient was imposed by lowering the temperature of one of the lower corners, rather than by increasing the temperature of the opposite corner. The amount was by about 10 percent of the total vertical temperature difference, and hence if the opposite had been done, the magnitude of the thermal Rayleigh number would have been effectively decreased by about 10 percent on the warmed side – which would have increased the instability by itself, even without the presence of the induced circulation. We emphasize that such was not the case here.

The computer resources, required for the simulations here, were rather large (similar to those of the previous section) since they were performed before improvements in the computer code, such as implicit differencing of the diffusion terms, were made. Some of these improvements were made on the infinite channel code, and the improvement in efficiency (reviewed in the next section) was quite dramatic.

It would be quite useful to have detailed experimental results of the configuration studied in this section, for the purpose of rigorous validation of computer codes. Previous laboratory studies of salt fingers have been made by producing the fingers at an interface between hot salty water above cold fresh water, rather than having linear gradients of heat and salt through the entire depth. To construct a basic state of the latter type would be much more difficult.

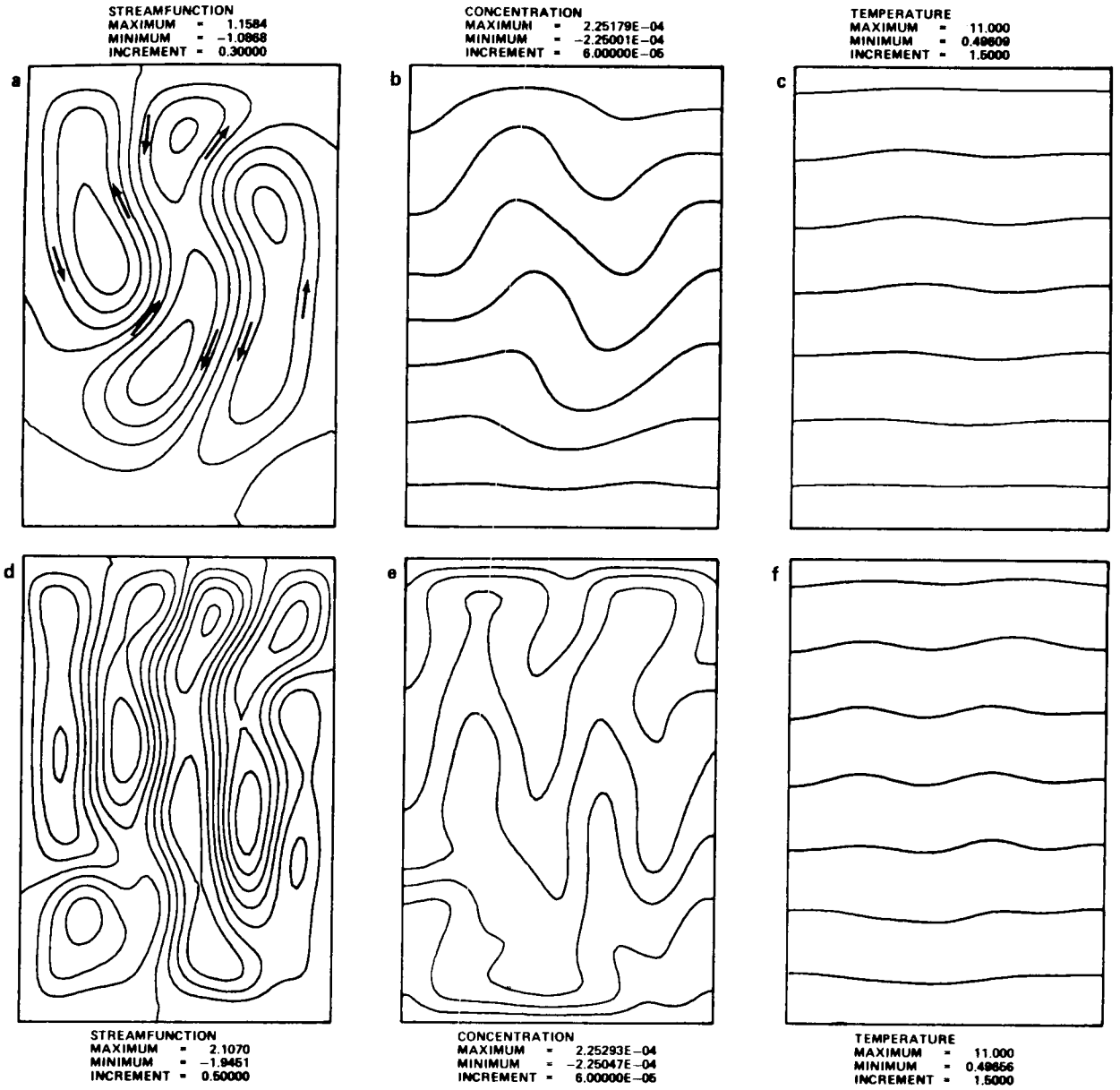

Figure 9. (a), (b), and (c): Results of calculations for case 1 of Section III at 1050 sec. (See text for details.) (d), (e), and (f): Results of calculations for case 1 of Section III at 700 sec.

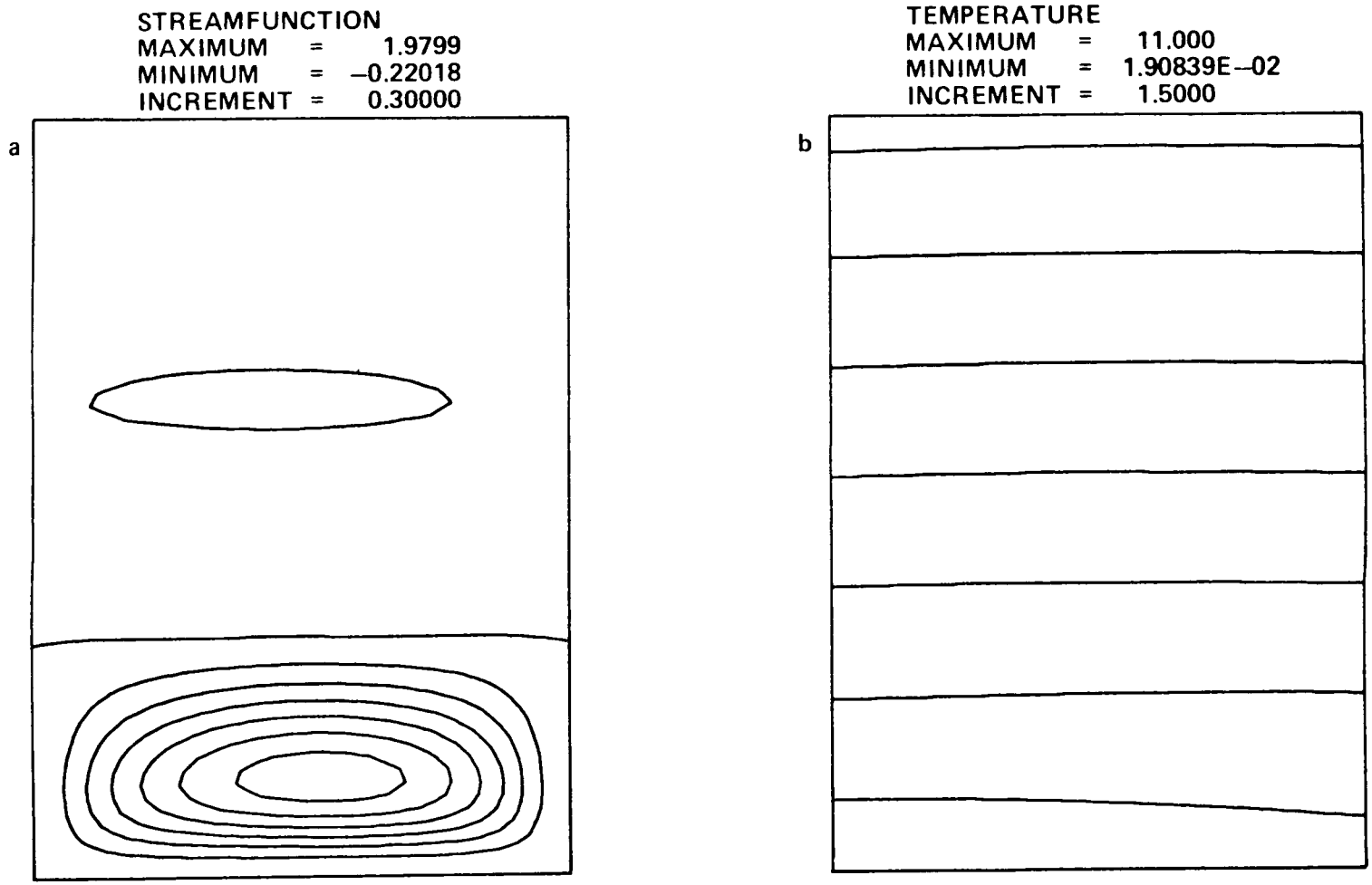

Figure 10. Results of calculations for case 3 of Section III. A horizontal temperature gradient is imposed upon the bottom surface. The horizontal temperature difference is 0.1 of the vertical difference imposed. There is no solute present.

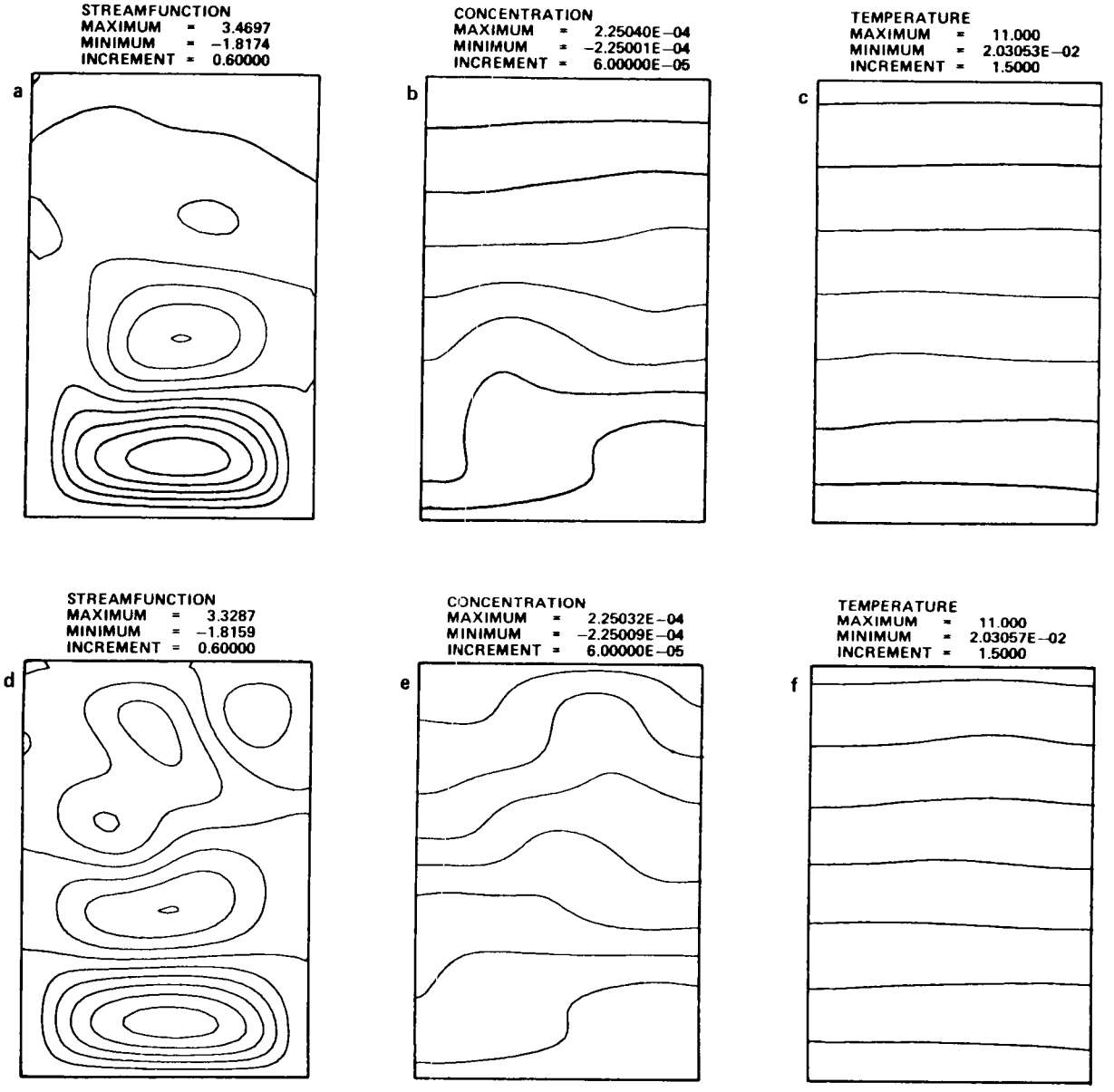

Figure 11. Results of calculations for case 4 of Section III at 300 sec (a, b, and c) and at 525 sec (d, e, and f).

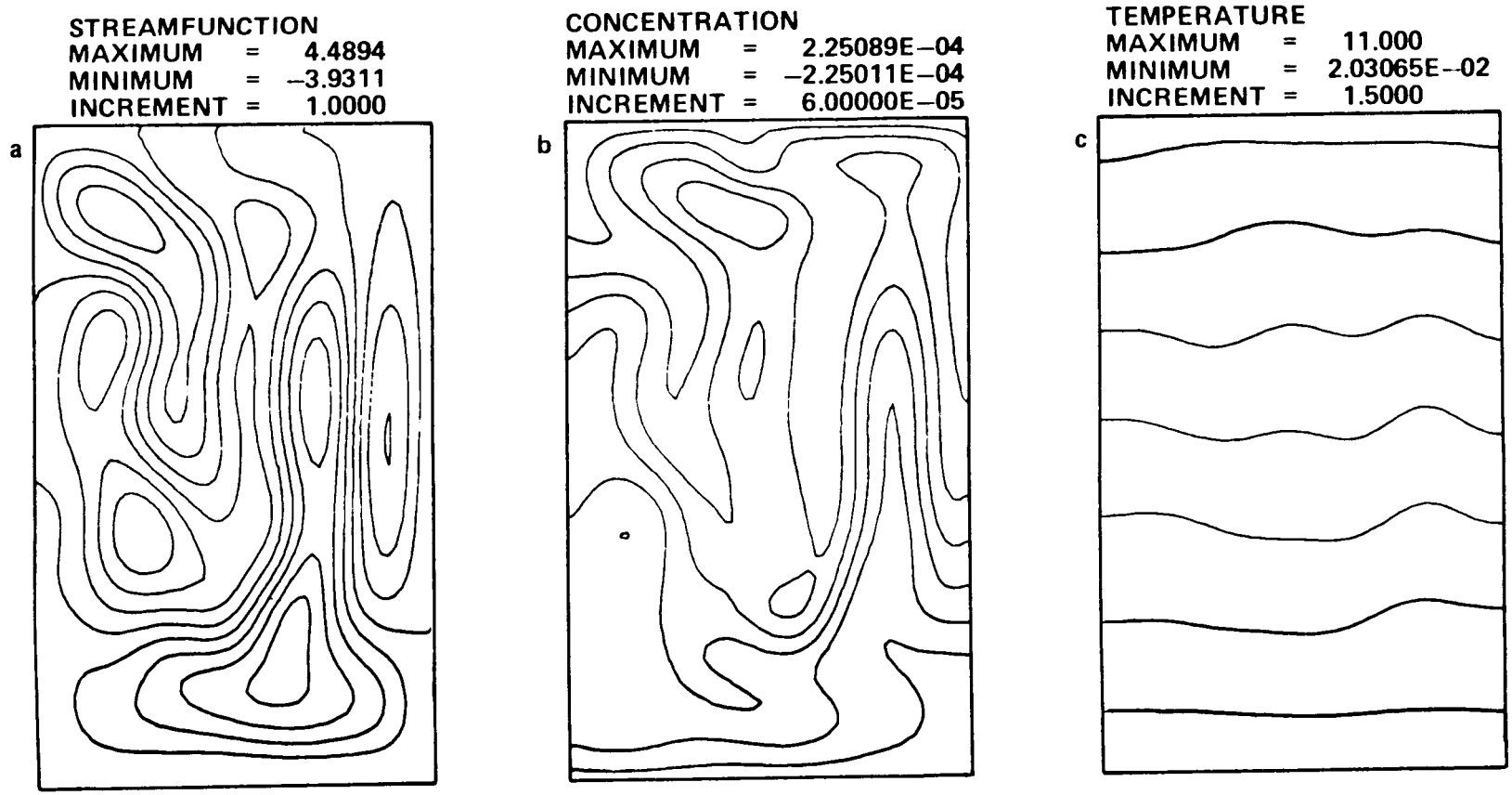

Figure 12. Results of calculations for case 5 of Section III at 175 sec.

In conclusion, there is evidence here that the always-present horizontal temperature gradients in the Bridgman-Stockbarger system may actually contribute to, rather than suppress, finger-type convection. Thus, any full simulation of the crystal growth situation where a light solute becomes concentrated at the interface must allow for the possibility of this relatively fine-scale convection. (That is, the resolution must be rather fine.) It is noted also that, due to the observation of the experimental works relating to the previous section, fingers may appear between horizontal convective layers when the overall solutal gradient is stable, and that this may occur in a crystal growing situation as well.

IV. FINGER CONVECTION IN THE INFINITE CHANNEL

The calculations presented here were performed as part of an effort to monitor a contract to demonstrate the performance of a spectral model on areas of relevance to crystal growth. The performance of the finite difference model here will eventually be compared with the performance of the spectral model. Free-slip conditions were taken on the horizontal boundaries, because the spectral model was based upon this condition and converting the spectral model to no-slip would not have been a trivial effort. The problem is essentially the same as that considered by Straus [18], although Straus assumed very small solutal diffusion compared with thermal and viscous diffusion, and thus simplified the equations. We have made no such simplification. The model here was based upon that of Miller [25] which is similar to the one used in the previous section with the following exceptions: boundary conditions on the vertical end walls are taken to be periodic. Solution of the Poisson equation [equation (2)] was by Fourier analysis in the horizontal and direct Gaussian elimination in the vertical. Improvements upon the model described in Miller [25] are as follows. The finite differencing of the vertical part of the temperature field was done implicitly (Crank-Nicholson), greatly improving the efficiency of the model for the PR < 1 cases reported here. (For the Pr = 0.1 cases, the allowable time step was increased by a factor of three.) Further improvement would have been achieved if the viscous diffusion term had also been differenced implicitly, and if ADI methods had been implemented to allow implicit differencing in the horizontal. Allowance was made for the time steps to be different for the vorticity, temperature, and concentration prediction equations. In the steady state situations studied here, this resulted in considerably fewer time steps required for convergence. This is because the small diffusivity of solute would otherwise require integration for a very long time in order to achieve equilibration. The improvement factor in computing the solutal Nusselt number to the degree of accuracy in Table 2 is about equal to the Schmidt number (10). These improvements were suggested by previous work of Dr. Glyn Roberts of Roberts Associates, Inc. (Roberts et al., [32]). The number of time steps for the coarser resolution reported here was about 2000 for "complete" convergence (constant solutal Nusselt number to 5 digits), which took about 4 min of CPU time on the UNIVAC 1180. Before the improvements were made to the code, this calculation would have taken about 2 hr.

Initial conditions were of diffusive equilibrium, but with a perturbation added to the solutal concentration field. The perturbation was in the form of a complete sine wave in the horizontal and a half sine wave in the vertical, of size 0.01.

Results are shown for Pr = 0.1 and Sc = 10. The length scale used in defining the Rayleigh numbers in these cases is the vertical depth of the channel. When the solutal Rayleigh number is super-critical enough that the flow is substantially nonlinear, this results in a moderately difficult problem for the numerical models, with a factor of 100 separating the two extreme diffusivities – although the diffusivities are not as extreme as in a true crystal growing situation. In that case, the Prandtl number would be about 0.01 (for liquid metals), and the Schmidt number would be between 100 and 1000. The assumption of periodic end wall conditions is also a great simplification over a more realistic domain (such as that in the previous section); only one horizontal wavelength is modeled here and hence fewer grid points are required. The results are reported by plotting the fields, plotting energy versus time, and by giving the solutal Nusselt

TABLE 2. NUSSELT NUMBER

Case	Ra_T	Ra_S	P	Sc	L[1]	Grid	Nu_S[2]
1a	-1000	- 90.9	0.1	10.	2.828	12 x 10	3.548
1b	-1000	- 90.9	0.1	10.	2.828	16 x 24	3.544
2	-1000	-100	0.1	10.	2.828	12 x 10	3.68
3	-1000	-100	0.1	10.	1.95	12 x 10	3.74 (3.74)
4	-1000	-200	0.1	10.	1.58	12 x 10	4.83 (4.85)
5	-1000	-300	0.1	10.	1.47	12 x 10	5.58 (5.62)
6	-1000	-400	0.1	10.	1.40	12 x 10	6.17

1. L is horizontal length of the computational domain, in terms of the vertical depth.
2. Numbers in parentheses are results from Straus [18].

number, which is the ratio of the resultant solutal flux through the boundaries to that of pure diffusion. Note that calculations have been performed only for cases where the resultant flow is steady. If the solutal Rayleigh number is increased enough, periodicity and chaos can ensue (S. A. Orszag, private communication, 1983).

The first case shown here is one that is only moderately super-critical. The thermal Rayleigh number was -1000 and the solutal Rayleigh number was -90.9. The critical Ra_S for this situation was about -76. The horizontal wavelength was $8^{1/2}$, which is the critical wavelength at the critical Ra_S. Figure 13 shows the vertical resolution of the two cases, along with the resultant average concentration profiles. The horizontal resolution was 12 intervals for the first case (Fig. 13a) and 16 intervals for the other. The number of vertical intervals was 10 and 24, respectively (the size of which was smoothly varied within the vertical extent of the domain). No qualitative differences are apparent between the two resolutions, and quantitative differences are small. In particular, the solutal Nusselt number (which would be expected to be rather sensitive to the resolution differences) is 3.548 and 3.544, respectively. Thus, the seemingly coarse resolution of 12 x 10 performs rather well, although the reader is reminded that the grid is stretched in the vertical, so that the resolution near the boundary is increased from that of a constant grid. In Figure 14 are plots of the fields at steady state for the coarser resolution case. The flow consists of convection cell extending the entire height of the domain. The temperature field deviates only slightly from the conduction state, and the solutal field is highly deformed. Note from Figure 13 that the horizontally averaged concentration field actually has a reversed vertically gradient in the middle of the domain.

Figure 15 shows the contour plots (at the coarse resolution) for the case with $Ra_S = 300$, which results in a more highly nonlinear flow. Note that the solutal perturbation is much larger, and that the convection cells are less symmetric with respect to the vertical. From the contour plot of concentration, it is evident that the resolution is beginning to be suspect, but the Nu_S comparison with Straus [18] is still quite good.

In summary, great improvements in computer usage efficiency can be made with the use of implicit methods in the diffusion terms and, for steady state solutions, with the use of different time steps for the different prediction equations. Furthermore, calculations of this configuration demonstrate the accuracy

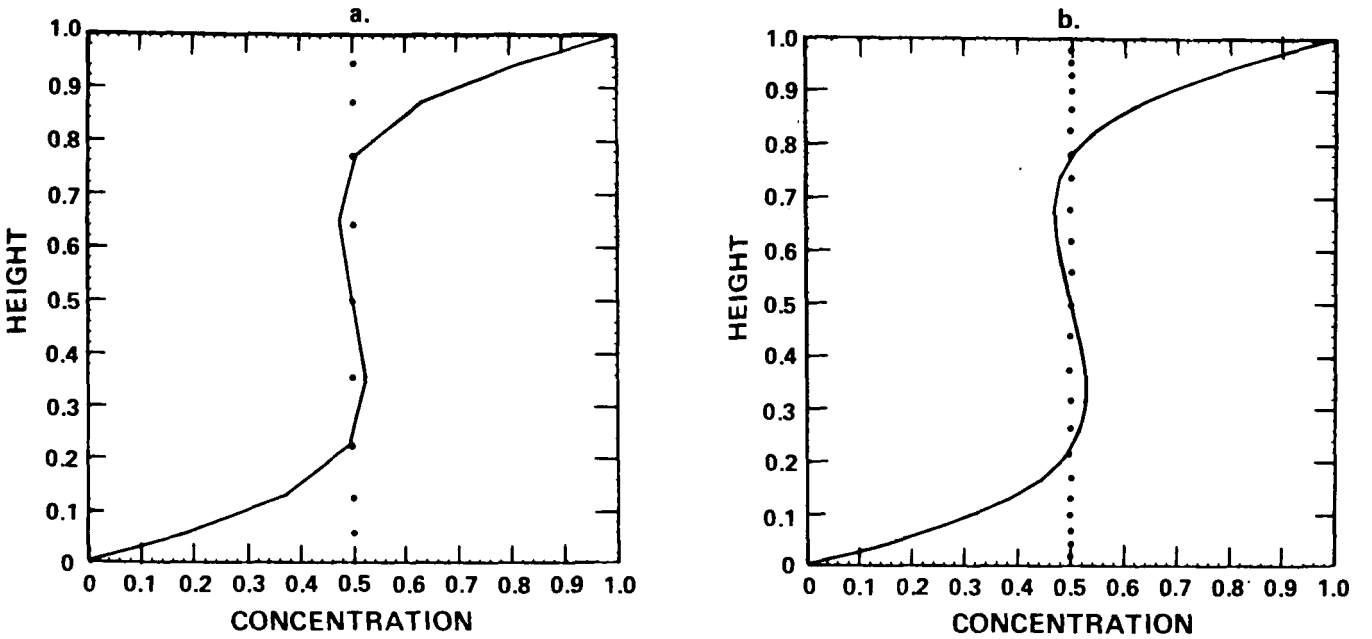

Figure 13. Calculated horizontally-averaged solutal concentration field as a function of height of two resolutions of case 1 of Section IV (Table 2). The discrete points indicate the vertical grid used in the calculations.

of the grid stretching method and difference scheme, since the results compare very well with the spectral calculations of Straus [18], even for the low resolution grid. As previously noted, however, these calculations are for a single convection cell, and for multiple cells the resolution would have to be increased appropriately.

V. CONCLUSIONS AND DISCUSSION

The calculations here indicate both the potential and shortcomings of finite difference methods for modeling thermosolutal convection. The shortcomings are not unique to finite difference methods, but would exist for finite element and spectral techniques as well – although the degree of shortcomings of each method is a subject for debate. The difficult aspect of modeling the full nonlinear flow is that thermosolutal convection tends to be of fine scale, due to a low-diffusivity component. This results in the need for many degrees of freedom in order to accurately describe the flow. Furthermore, the existence of higher-diffusivity components results in time step restrictions (which may be quite severe, due to the fine resolution), unless implicit methods are used. (Note that all three methods almost invariably use finite differencing in time.) Implicit methods in the finite difference context have the advantage of being easier to implement than for the other two methods.

The flows calculated here certainly reinforce the expectation that double-diffusive convection is important in crystal growing systems, although much more work is needed before this is shown to be a fact. Certainly it is reasonable to expect that thermosolutal convection is important when there is a tendency for a light component to be present near the bottom of the liquid, even when the liquid is cooled from below. This is the "salt finger" situation. Furthermore, even when the solutal contribution is to make the system bottom-heavy, horizontal temperature gradients, if they are strong enough, can conceivably drive a flow which causes horizontal layering and subsequent overturning of the solute (c.f., Section II). Experimental results have indicated that finger convection can then occur within the individual convection cells. Computations of this phenomenon were not performed, due to the very high resolution that would be required.

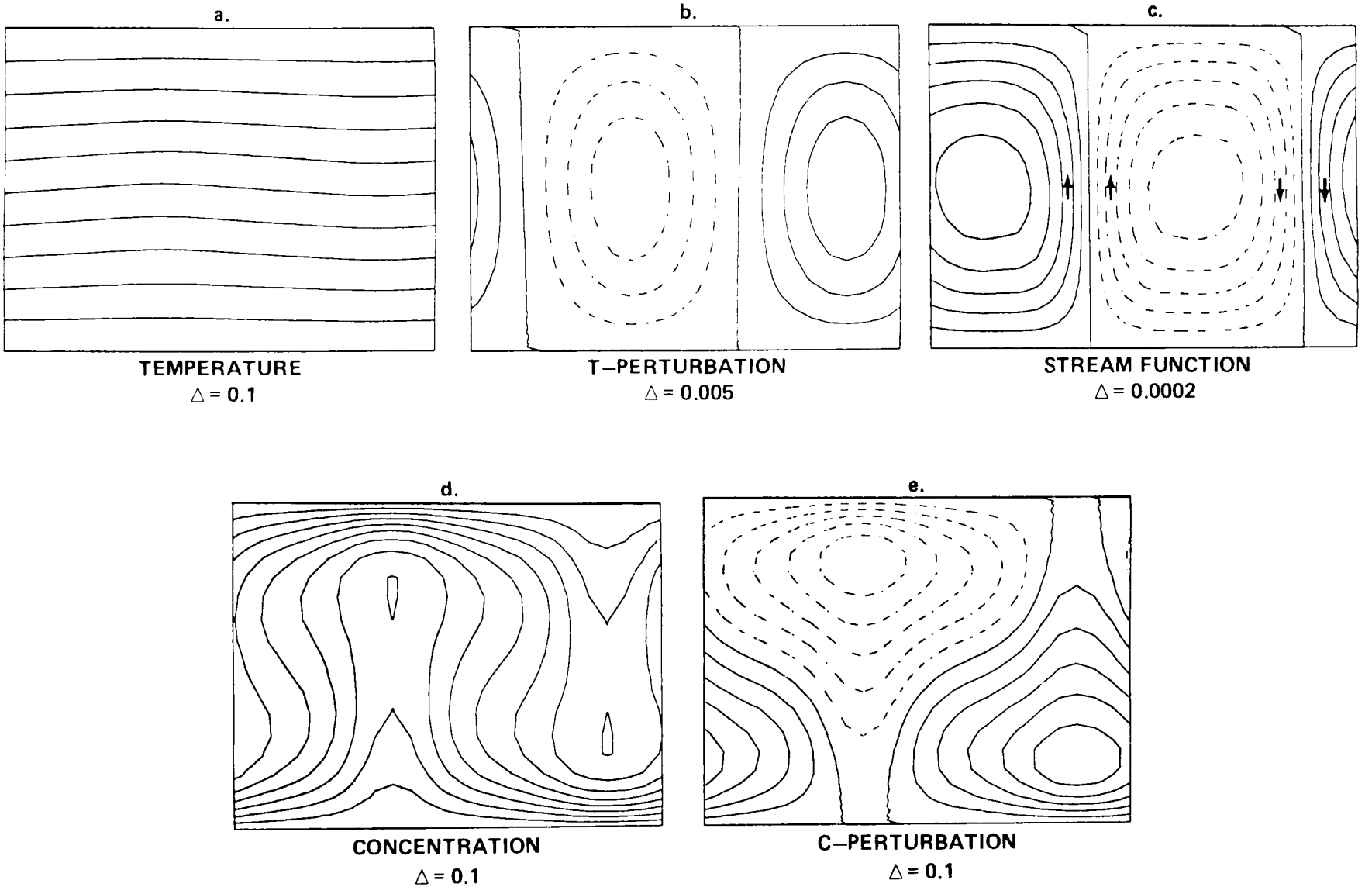

Figure 14. Contour plots of the calculated fields for case 1a of Section IV (Table 2).

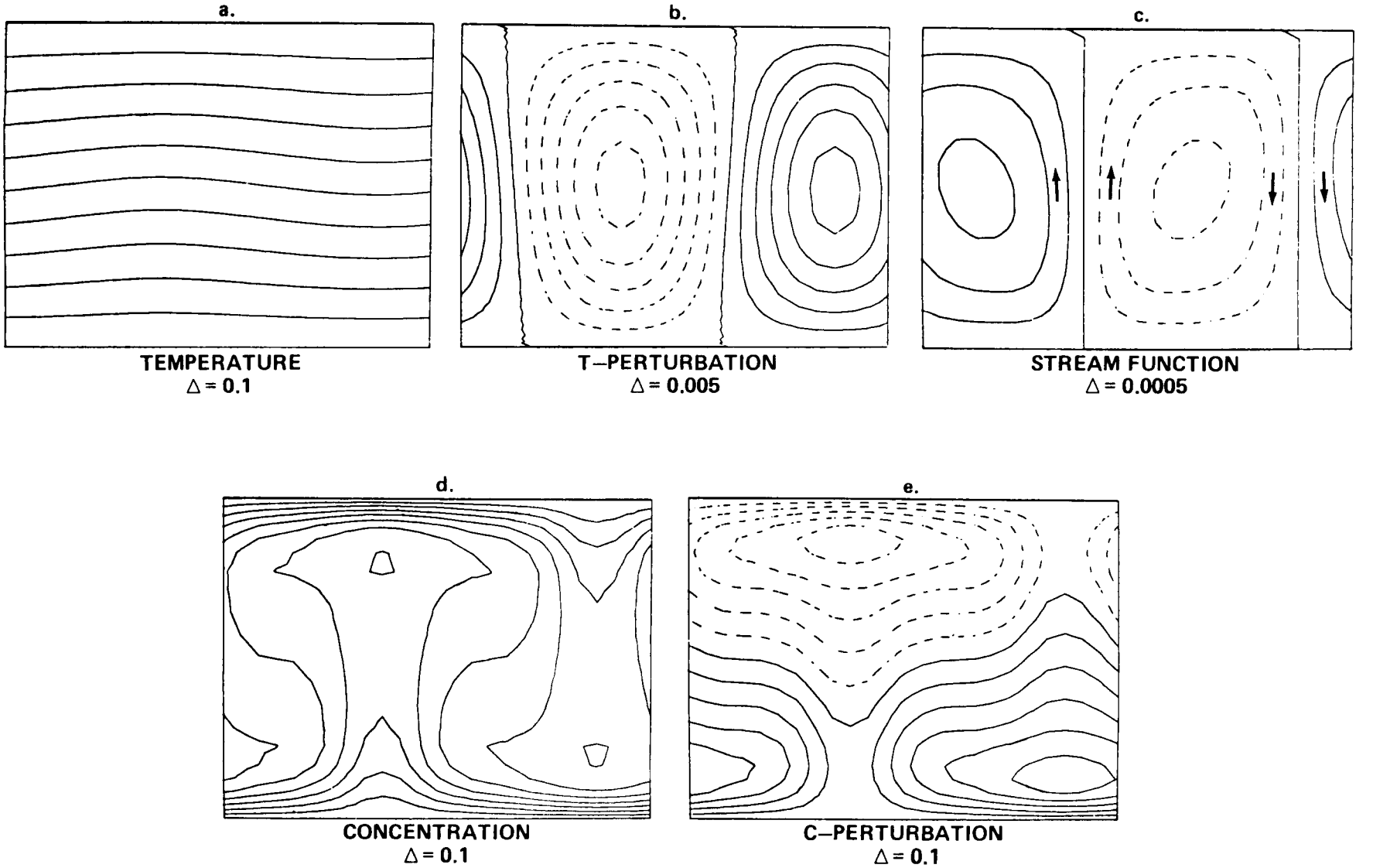

Figure 15. Contour plots of the calculated fields for case 5 of Section IV (Table 2).

The main aspects of the crystal growing situations that were neglected here are: (1) possibly curved lower boundary; (2) a basic growth flow through the system, which results in exponential rather than linear background states; (3) cylindrical geometric effects; and (4) three-dimensional effects. To fully include all of these effects would indeed be a giant step forward in the modelling of crystal growth. The first three effects are included in the crystal growth modelling efforts of the groups mentioned in the introduction. (Including fully three-dimensional effects may not be a realistic goal, even with the use of the latest generation of super-computers – at least when thermosolutal convection is present.) The primary common weakness of those efforts mentioned is that they did not fully include the thermosolutal effects studied here. It is hoped that the present work will assist crystal growth modellers by pointing out the extent of some of the resolution and other numerical problems facing them in order to have a complete description of the fluid dynamics of the melt, and hence of the crystal itself.

REFERENCES

1. Turner, J. S.: Buoyancy Effects in Fluids. London, Cambridge University Press, 1973.

2. Coriell, S. R., Cordes, M. R., and Boettinger, W. J.: Convective and Interfacial Instabilities During Unidirectional Solidification of a Binary Alloy. J. Crystal Growth, Vol. 49, 1980, pp. 13-28.

3. Thorpe, S. A., Hutt, P. K., and Soulsby, R.: The Effect of Horizontal Gradients on Thermohaline Convection. J. Fluid Mech., Vol. 38, 1969, pp. 375-400.

4. Chen, C. F., Briggs, D. G., and Wirtz, R. A.: Stability of Thermal Convection in a Salinity Due to Lateral Heating. Int. J. Heat Mass Transfer, Vol. 14, 1971, pp. 57-65.

5. Wirtz, R. A., Briggs, D. G., and Chen, C. F.: Physical and Numerical Experiments on Layered Convection in a Density-Stratified Fluid. Geophys. Fluid Dyn., Vol. 3, 1972, pp. 265-288.

6. Wirtz, R. A., and Liu, L. H.: Numerical Experiments on the Onset of Layered Convection in a Narrow Slot Containing a Stably Stratified Fluid. Int. J. Heat Mass Trans., Vol. 18, 1975, pp. 1299-1305.

7. Wirtz, R. A.: The Effect of Solute Layering on Lateral Heat Transfer in an Enclosure. Int. J. Heat Mass Trans., Vol. 20, 1977, pp. 841-846.

8. Chen, C. F., and Johnson, D. H.: Double-Diffusive Convection: A Report on an Engineering Foundation Conference. J. Fluid Mech., Vol. 138, 1984, pp. 405-416.

9. Stommel, H., Arons, A. B., and Blanchard, D.: An Oceanographic Curiosity: The Perpetual Salt Fountain. Deep-Sea Res., Vol. 3, 1956, pp. 152-153.

10. Stern, M. E.: The "Salt-Fountain" and Thermohaline Convection. Tellus, Vol. 12, 1960, pp. 172-175.

11. Walin, G.: Note on the Stability of Water Stratified by Salt and Heat. Tellus, Vol. 16, 1964, p. 389.

12. Schmitt, R. W.: The Growth Rate of Super-Critical Salt Fingers. Deep-Sea Res., Vol. 26A, 1979, pp. 23-40.

13. Veronis, G.: On Finite Amplitude Instability in Thermohaline Convection. J. Mar. Res., Vol. 23, 1965, pp. 1-17.

14. Veronis, G.: Effect of a Stabilizing Gradient of Solute on Thermal Convection. J. Fluid Mech., Vol. 34, 1968, pp. 315-336.

15. Sani, R. L.: On Finite-Amplitude Roll Cell Disturbances in a Fluid Layer Subjected to a Heat and Mass Transfer. Am. Inst. Chem. Eng. J., Vol. 11, 1965, pp. 971-980.

16. Huppert, H. E., and Moore, D. R.: Nonlinear Double-Diffusive Convection. J. Fluid Mech., Vol. 78, 1976, pp. 821-854.

17. Moore, D. R., Toomre, J., Knobloch, E., and Weiss, N. O.: Period Doubling and Chaos in Partial Differential Equations for Thermosolutal Convection. Nature, Vol. 303, 1983, pp. 663-667.

18. Straus, J. M.: Finite Amplitude Doubly Diffusive Convection. J. Fluid Mech., Vol. 56, 1972, pp. 353-374.

19. Carlson, F. M., Fripp, A. L., and Crouch, R. K.: Thermal Convection During Bridgman Crystal Growth. J. Crystal Growth, 1984, in press.

20. Schaefer, R. J., Coriell, S. R., McFadden, G. B., and Rehm, R. G.: Convection During Unidirectional Solidification. In National Bureau of Standards Report NBSIR 82-2560, J. R. Manning, editor, 1982.

21. Chang, C. J., and Brown, R. A.: Radial Segregation Induced by Natural Convection and Melt/Solid Interface Shape in Vertical Bridgman Growth. J. Crystal Growth, Vol. 63, 1983, pp. 22-43.

22. Brown, R. A., Chang, C. J., and Adornato, P. M.: Finite Element Analysis of Directional Solidification of Dilute and Concentrated Binary Melts. In Modeling of Casting and Welding Processes (J. A. Dantzig and J. T. Berry, eds.), AIME, 1984 (in press).

23. Miller, T. L., and Gall, R. L.: Thermally Driven Flow in a Rotating Spherical Shell. J. Atmos. Sci., Vol. 40, 1983, pp. 856-868.

24. Miller, T. L., and Gall, R. L.: A Linear Analysis of the Transition Curve for the Baroclinic Annulus. J. Atmos. Sci., Vol. 40, 1983, pp. 2293-2303.

25. Miller, T. L.: The Structures and Energetics of Symmetric Baroclinic Waves. J. Fluid Mech., Vol. 142, 1984, pp. 343-362.

26. Hart, J. E.: Finite Amplitude Sideways Diffusive Instability. J. Fluid Mech., Vol. 59, 1973, pp. 47-64.

27. Ruddick, B. R., and Turner, J. S.: The Vertical Length Scale of Double-Diffusive Intrusions. Deep-Sea Res., Vol. 26A, 1979, pp. 903-913.

28. Hart, J. E.: On Sideways Diffusive Instability. J. Fluid Mech., Vol. 49, 1971, pp. 279-288.

29. Chen, C. F.: Onset of Cellular Convection in a Salinity Gradient Due to a Lateral Temperature Gradient. J. Fluid Mech., Vol. 63, 1974, pp. 563-576.

30. Holyer, J. Y.: Double-Diffusive Interleaving Due to Horizontal Gradients. J. Fluid Mech., Vol. 137, 1983, pp. 347-362.

31. Baines, P. G., and Gill, A. E.: On Thermohaline Convection with Linear Gradients. J. Fluid Mech., Vol. 37, 1969, pp. 289-306.

32. Roberts, G. O., Fowlis, W. W., and Miller, T. L.: Finite-Difference Fluid Dynamics Computer Mathematical Models for the Design and Interpretation of Experiments for Space Flight. NASA Technical Paper 2323, May 1984.

1. REPORT NO.	2. GOVERNMENT ACCESSION NO.	3. RECIPIENT'S CATALOG NO.
NASA TP -2394		

4. TITLE AND SUBTITLE	5. REPORT DATE
A Preliminary Study of Numerical Simulation of Thermosolutal Convection of Interest to Crystal Growth	November 1984
	6. PERFORMING ORGANIZATION CODE
7. AUTHOR(S)	8. PERFORMING ORGANIZATION REPORT #
Timothy L. Miller	
9. PERFORMING ORGANIZATION NAME AND ADDRESS	10. WORK UNIT NO.
George C. Marshall Space Flight Center Marshall Space Flight Center, Alabama 35812	M-465
	11. CONTRACT OR GRANT NO.
	13. TYPE OF REPORT & PERIOD COVERED
12. SPONSORING AGENCY NAME AND ADDRESS	Technical Paper
National Aeronautics and Space Administration Washington, D.C. 20546	14. SPONSORING AGENCY CODE

15. SUPPLEMENTARY NOTES

Prepared by Space Science Laboratory, Science and Engineering Directorate.

16. ABSTRACT

Calculations have been performed with computer models using three types of finite difference methods of thermosolutal convection: horizontal heating of a container filled with a stably stratified solution, finger convection in a container, and finger convection in a horizontally infinite channel. The importance of including thermosolutal convection in models of crystal growth is emphasized, and the difficulties in doing so are demonstrated. It is pointed out that these difficulties, due primarily to the fine structure of the convection, may be partly overcome by the use of fine grids and implicit time stepping methods.

17. KEY WORDS	18. DISTRIBUTION STATEMENT
Thermosolutal Convection Crystal Growth Double Diffusive Numerical Modeling of Fluid Flow	Unclassified - unlimited Subject Category: 34

19. SECURITY CLASSIF. (of this report)	20. SECURITY CLASSIF. (of this page)	21. NO. OF PAGES	22. PRICE
Unclassified	Unclassified	33	A03

For sale by National Technical Information Service, Springfield, Virginia 22161

NASA-Langley, 1984

7 2 1U,D, 841120 S00161DS
DEPT OF THE AIR FORCE
ARNOLD ENG DEVELOPMENT CENTER(AFSC)
ATTN: LIBRARY/DOCUMENTS
ARNOLD AF STA TN 37389